Journal of Hepatocellular Carcinoma

Dovepress
open access to scientific and medical research

Open Access Full Text Article

ORIGINAL RESEARCH

Integration of Multimodal Computed Tomography Radiomic Features of Primary Tumors and the Spleen to Predict Early Recurrence in Patients with Postoperative Adjuvant Transarterial Chemoembolization

Cong Chen[1,*], Jian Liu[2,*], Zhuxin Gu[1], Yanjun Sun[1], Wenwu Lu[3], Xiaokan Liu[4], Kang Chen[1], Tianzhi Ma[5], Suming Zhao[1], Hui Zhao[1]

[1]Department of Interventional & Vascular Surgery, Affiliated Hospital of Nantong University, Nantong, 226001, People's Republic of China; [2]Dalian Medical University and Affiliated Hospital of Nantong University, Nantong, 226001, People's Republic of China; [3]Department of Medical Ultrasound, Affiliated Hospital of Nantong University, Nantong, 226001, People's Republic of China; [4]Department of Interventional Radiology, Affiliated Hospital 2 of Nantong University, Nantong, 226001, People's Republic of China; [5]Nanjing University of Aeronautics and Astronautics, Nanjing, 210000, People's Republic of China

*These authors contributed equally to this work

Correspondence: Suming Zhao; Hui Zhao, The Affiliated Hospital of Nantong University, No. 20, Xisi Road, Chongchuan District, Nantong City, Jiangsu Province, People's Republic of China, Tel +86-513-85052071, Email 5201120@ntu.edu.cn; zhaohui8868@sina.com

Background: Hepatocellular carcinoma (HCC) is one of the most lethal malignancies in the world. Patients with HCC choose postoperative adjuvant transarterial chemoembolization (PA-TACE) after surgical resection to reduce the risk of recurrence. However, many of them have recurrence within a short period.

Methods: In this retrospective analysis, a total of 173 patients who underwent PA-TACE between September 2016 and March 2020 were recruited. Radiomic features were derived from the arterial and venous phases of each patient. Early recurrence (ER)-related radiomics features of HCC and the spleen were selected to build two rad-scores using the least absolute shrinkage and selection operator (LASSO) Cox regression analysis. Logistic regression was applied to establish the Radiation (Rad)_score by combining the two regions. We constructed a nomogram containing clinical information and dual-region rad-scores, which was evaluated in terms of discrimination, calibration, and clinical usefulness.

Results: All three radiological scores showed good performance for ER prediction. The combined Rad_score performed the best, with an area under the curve (AUC) of 0.853 (95% confidence interval [CI], 0.783–0.908) in the training set and 0.929 (95% CI, 0.789–0.988) in the validation set. Multivariate analysis identified total bilirubin (TBIL) and the combined Rad_score as independent prognostic factors for ER. The nomogram was found to be clinically valuable, as determined by the decision curves (DCA) and clinical impact curves (CIC).

Conclusion: A multimodal dual-region radiomics model combining HCC and the spleen is an independent prognostic tool for ER. The combination of dual-region radiomics features and clinicopathological factors has a good clinical application value.

Keywords: hepatocellular carcinoma, radiomics, nomogram, transcatheter arterial chemoembolization, computed tomography

Introduction

Hepatocellular carcinoma (HCC) is the sixth most common malignancy worldwide and is characterized by high incidence, poor prognosis, and high mortality.[1] Hepatocellular carcinoma is the most common type of liver cancer.[2] Most patients with hepatocellular carcinoma have progressed to intermediate and advanced stages by the time they are diagnosed, missing the

Received: 27 May 2023
Accepted: 28 July 2023
Published: 8 August 2023

best time to receive surgical treatment, while the one-year survival rate of untreated patients with intermediate and advanced HCC is only 17.5%.[3] With the improvement in HCC treatment, various treatment options such as liver transplantation, surgical resection, systemic therapy, and liver-targeted therapy have become available. However, surgical treatment is still considered the primary treatment modality for hepatocellular carcinoma.[4] However, the high tumor recurrence rate is the leading cause of postoperative death in patients with HCC, and the 5-year recurrence rate can be as high as 75%-100%.[5]

Transarterial chemoembolization (TACE) has a critical role in the treatment of HCC as a stand-alone or combination therapy in each stage of HCC.[6] According to the American Society for the Study of Liver Diseases (AASLD) and European Association for the Study of the Liver (EASL) guidelines, TACE is the first choice of treatment for multiple HCC.[7–9] For BCLC stage B (intermediate HCC), TACE is the standard treatment.[6] Chinese Consensus-Based Interdisciplinary Expert Statements believed that TACE combination including targeted/immunotherapy, radiotherapy, and liver transplantation can further improve the survival benefits of HCC patients.[9] Postoperative adjuvant TACE (PA-TACE) detects and treats postoperative residual foci and early recurrent foci rapidly. Many guidelines recommend adjuvant TACE after hepatectomy without definite detection of tumor recurrence to enhance the outcome of hepatocellular carcinoma surgery;[10] however, it has a limited role in preventing distant neoplastic hepatocellular carcinoma. Improvements have been made to the infusion of drugs and iodinated oil during TACE surgery to further enhance the long-term efficacy of TACE and prolong the occurrence of TACE resistance.[11,12] Wang et al retrospectively analyzed 271 HCC patients and found that PA-TACE was a safe intervention and could effectively prevent tumor recurrence.[13] Chen et al retrospectively analyzed nearly 2000 HCC patients and found that PA-TACE did not delay or avoid distant recurrence of HCC.[14] Rapid detection of early recurrence (ER) can be an intervention for patients with hepatocellular carcinoma who have already undergone surgical resection to prolong survival as much as possible. Therefore, predicting ER is important in patients undergoing PA-TACE. One year is the best interval to determine early and late intrahepatic recurrence after hepatectomy for hepatocellular carcinoma.[15,16] In this study, ER was defined as new intrahepatic lesions or distant metastases that appeared within the liver one year after hepatectomy for hepatocellular carcinoma.

Radiomics, based on radiomic data extracted from medical images and subsequent data analysis, has led to significant advances in cancer research, such as disease surveillance, diagnosis, prognosis, and treatment response prediction.[17,18] A large body of literature shows that computed tomography (CT) image-based radiomic analysis has been successfully used to predict individual survival in HCC.[19–21] However, a significant limitation of these studies is that the radiomic signature is focused only on the primary tumor, and most of them were performed in only one phase. Li et al utilized radiomic characterization of the spleen to predict potential biological markers of early and late recurrence of HCC after surgery.[16] Primary tumors in HCC patients can promote tumor progression and metastasis by inducing inflammation and regulating the spleen (immunosuppression to promote tumor progression).[22,23] Wang et al demonstrated that the splenic imaging model was an independent risk factor for survival in patients with gastric cancer,[24] and that spleen density could predict the overall survival of patients with gastric cancer.[25] These results indicate that the spleen is closely associated with the development of primary tumors. It is reasonable to believe that changes in the spleen may reflect HCC progression to some extent. The advantage of using splenic imaging features is that they are not affected by the size of the primary tumor and can be easily obtained by simple treatment prior to surgery. To our knowledge, there are no studies on the prognostic value of combined primary tumor and spleen radiomic sign maps for postoperative PA-TACE in patients with hepatocellular carcinoma.

This retrospective analysis sought to evaluate whether dual-regional signals of the primary tumor and spleen in CT images could provide a higher prognostic value than the existing single radiomic signal in predicting ER after postoperative PA-TACE in patients with HCC. It is hoped that the radiomic nomogram established and validated in this study will provide new options for clinical decision-making.

Materials and Methods

Study Population

This retrospective study was approved by the ethical review committee of the Affiliated Hospital of Nantong University, which waived the requirement for informed consent. The ethical review number for this project was 2022-K090-01. For the dataset, we evaluated the Affiliated Hospital of Nantong University medical record database between September 2016

and March 2020 to identify patients with histologically confirmed hepatocellular carcinoma who had undergone surgical resection. The patient inclusion criteria were as follows: (1) pathologically confirmed primary liver cancer; (2) no tumor recurrence or metastasis before postoperative TACE; (3) plain and enhanced scan within one week before liver resection; (4) no treatment such as drugs and radiotherapy before CT examination; and (5) no contraindication to CT-enhanced scanning examination, such as contrast allergy, hyperthyroidism, or asthma. Patient exclusion criteria included (1) recurrent hepatocellular carcinoma, (2) patients receiving other treatments (including radiotherapy, targeted drug therapy, etc.) after hepatectomy, (3) patients with splenectomy and incomplete spleen scan, (4) patients with low image quality to meet diagnostic requirements, (5) patients with small lesions that make it challenging to outline the area of interest, and (6) patients who were lost follow-up or missing clinical information. The flowchart for screening the study population is shown in Figure 1A. Patients who met the inclusion criteria were randomly assigned to training and validation groups at a ratio of 8:2. The training and validation groups included 138 and 35 patients, respectively.

Clinical and Pathological Data

All the patients underwent radical surgery for primary hepatocellular carcinoma. Reviewing the Hospital Information System (HIS), we retrieved basic information about the patients the week before radical hepatocellular carcinoma surgery, including sex, age, tumor size, hepatitis, and serologic test indicators. Serological data included alanine transaminase (ALT), aspartate aminotransferase (AST), total bilirubin (TBIL), alpha-fetoprotein (AFP), prothrombin time (PT), and albumin (ALB). The operation and drug selection of PA-TACE in this study strictly follow the Chinese Guidelines for the Diagnosis and Treatment of Primary Liver Cancer (2022 edition)[26] and the Chinese Guidelines for Clinical Practice of Transcatheter Arterial Chemoembolization (TACE) for Hepatocellular Carcinoma (2021 edition).[27] The right femoral artery is punctured using the Seldinger method and the catheter is guided under fluoroscopy into the proper hepatic artery. The microcatheter was guided into each tumor-supplying artery using a micro guidewire after the intrinsic hepatic artery angiography. After perfusion chemotherapy with 2 mg raltitrexed and 100 mg oxaliplatin, 20 mg pirarubicin was mixed with 5 mL of iodinated oil to form an emulsion to act as chemoembolization of the arteries. The amounts of intraoperative chemotherapeutic medicines and iodinated oil were determined according to the patient's liver function, physical condition, body surface area, and other factors. All patients were followed up every

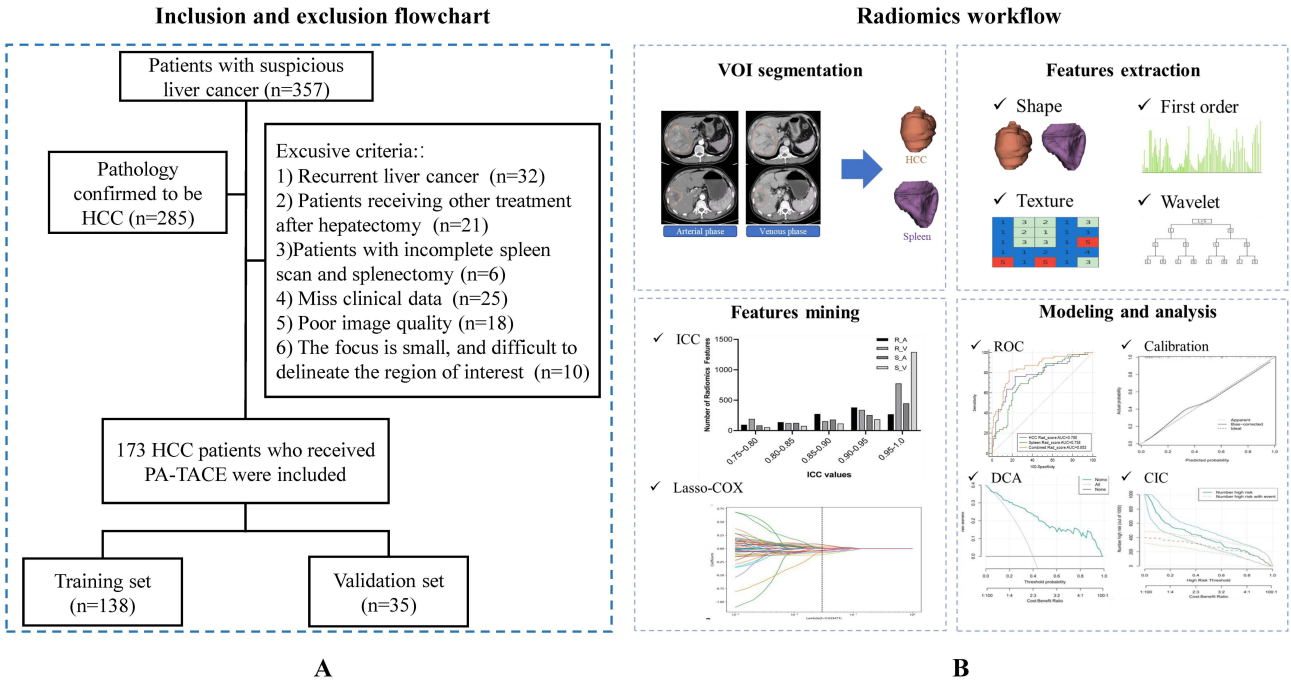

Figure 1 The study flowchart and the radiomics workflow. (**A**) Inclusion and exclusion flowchart of patients; (**B**) radiomics workflow.

3–6 months for two years after surgery, every six months in the third year after surgery, and annually in the fourth year and later. Imaging, including enhanced CT, magnetic resonance imaging (MRI), and ultrasound or pathological biopsy, was performed to clarify the diagnosis when patients were judged to have a possible recurrence based on a combination of factors, such as blood count and patient physical signs. According to the Modified Response Evaluation Criteria in Solid Tumors (mRECIST) criteria,[28] progressive disease (PD) was defined as ER within one year of hepatectomy in this study.

CT Imaging

All enrolled patients underwent an abdominal CT-enhanced scan (General Electric, GE) within one week before hepatectomy for hepatocellular carcinoma. Patients were placed in the supine position, and an abdominal scan was performed with inspiration and breath-holding. The scanning area was from the diaphragm to the lower edge of the liver. The CT scan parameters were as follows: 120 kV, 200 effective mAs, beam collimation 192×0.6 mm; 512×512 matrix, and pitch 0.8. Arterial, portal, and delayed phase scans were performed 25–30, 60–70, and 100–120 seconds after contrast injection. The contrast dose was 1.5–2mL/kg. After scanning, all image data were analyzed at the GE Symbia workstation.

The Volume of Interest Segmentation and Radiomics Features Evaluation

Tumor segmentation was performed by reader 1 (with six years of experience in diagnosing liver diseases). To consider feature robustness to intra- and inter-rater depiction changes, images of 50 patients were re-sketched by the same radiologist and another radiologist (with eight years of experience in liver disease diagnosis). Tumor segmentation was performed using the 3D slicer (version 5.0.3) software. Two readers manually depicted the tumor and spleen volume of interest (VOI) in the arterial and venous phases, layer by layer. Clinical information regarding the patient was not available in advance for either physician. To ensure consistent spatial resolution, we resampled all the CT images to 1 × 1×1 mm3 in all directions. After segmentation, we used the Pyradiomics package (version 3.0.1, https://pyradiomics.readthedocs.io/) to extract radiomic features from each 3D segmented region. Each region contained 3812 radiomics features, including 640 first-order intensity features, 499 shape features, and 2673 high-order texture features for both the arterial and venous phases in each VOI. Texture features were estimated using several methods, such as the gray-level co-occurrence matrix (GLCM), gray-level run length matrix (GLRLM), gray-level size zone matrix (GLSZM), and gray-level dependence matrix (GLDM).

Radiomics Feature Selection and Radiomics Signature Construction

To prioritize high-dimensional features, a three-step feature selection strategy was applied. First, the reproducibility of each feature was measured by calculating the intraclass correlation coefficient (ICC) within and between raters. Features with ICC < 0.75 were excluded from the subsequent analysis. We also conducted the Mann–Whitney *U*-test and feature screening for all radiomic features. Only radiomic features with a p-value < 0.05 were retained. Spearman's rank correlation coefficient was used to calculate the correlation between the features. Features with correlation coefficients greater than 0.9 were retained.

Finally, the least absolute shrinkage and selection operator (LASSO) regression model was used on the discovery dataset for signature construction. Depending on the regulation weight λ, LASSO shrinks all the regression coefficients toward zero and sets the coefficients of many irrelevant features to zero. To find the optimal λ, 10-fold cross-validation with minimum criteria was employed, where the final value of λ yielded the minimum cross-validation error. The retained features with nonzero coefficients were used for regression model fitting and were combined into a radiomics signature. Subsequently, we obtained a radiomics score for each patient using a linear combination of the retained features weighted by their model coefficients. The Python scikit-learn package was used for the LASSO regression modeling. Using this method, we constructed signatures of the tumor and spleen regions separately. Liver and spleen signatures were fused using logistic regression to build a dual-region joint model.

Validation and Comparison of the Radiomics Signatures

The most relevant clinical indicators of ER after PA-TACE were screened using univariate and multivariate logistic regression models. A nomogram was constructed by combining the imaging and clinical characteristics using logistic

regression. We used the receiver operating characteristic (ROC) curve to compare the performances of the combined models. The area under the curve (AUC) was calculated to quantify predictive power. The calibration curve and Hosmer-Lemeshow test were then used to verify the predictive performance of the nomogram. Decision curve analysis (DCA) and a clinical impact curve (CIC) were used to evaluate the net benefit of the nomogram in a clinical context.

Results

Patient Characteristics

The flow chart of this study is shown in Figure 1B.

Detailed clinicopathological data for the training and validation sets are summarized in Table 1 and Table 2. ER-positive patients accounted for 39.9% (55/138) and 40.0% (14/35) of the patients in the training and validation datasets, respectively. We analyzed the common clinical tests and found no significant differences between the two datasets (Table 1).

Univariate analysis showed that in the training group, tumor size (p=0.046), AST (p=0.004), and TBIL (p=0.003) were significantly different between patients with and without ER after PA-TACE, whereas the data from the remaining groups were not different. Similarly, in the validation group, the differences in tumor size (p=0.014), AST (p=0.017), and TBIL (p=0.02) were statistically significant between patients with and without ER after PA-TACE, whereas no significant differences were observed in the remaining indices (Table 2).

Table 1 Basic Characteristics of Enrolled Patients

Characteristic	Training Set (n=138)	Validation Set (n=35)	P-value
Sex			0.755
Male	107 (77.5)	28 (80)	
Female	31 (22.5)	7 (20)	
Age (years, mean ± SD)	56.46 ± 10.39	58.34 ± 10.74	0.342
Maximum tumor diameter (cm, mean ± SD)	5.0 ± 2.86	4.94 ± 3.56	0.908
ALBI grade			0.802
I	52 (37.7)	14 (40)	
II	86 (62.3)	21 (60)	
HBV			0.682
Positive	88 (63.8)	21 (60)	
Negative	50 (36.2)	14 (40)	
Cirrhosis			0.701
Positive	62 (44.9)	17 (48.6)	
Negative	76 (55.1)	18 (51.4)	
AFP (ng/mL)			0.962
≤20	67 (48.6)	13 (37.1)	
20–400	26 (18.8)	9 (25.8)	
≥400	45 (32.6)	13 (37.1)	
ALT (U/L, mean ± SD)	43.04 ± 37.91	53.14 ± 58.11	0.334
AST (U/L, mean ± SD)	43.05 ± 26.52	53.23 ± 50.35	0.255
PT (s, mean ± SD)	12.17 ± 1.69	11.73 ± 1.12	0.070
ALB (g/L, mean ± SD)	38.60 ± 3.86	39.02 ± 3.05	0.494
TBIL (μmol/L, mean ± SD)	16.79 ± 7.24	17.15 ± 10.21	0.847
HCC Rad_score (medians ± IQ)	0.37 ± 0.20	0.38 ± 0.25	0.876
Spleen Rad_score (medians ± IQ)	0.38 ± 0.07	0.39 ± 0.09	0.794
Combined Rad_score (medians ± IQ)	0.39 ± 0.52	0.42 ± 0.80	0.731

Note: Data are numbers of patients, and parentheses indicate the proportion if not specified.
Abbreviations: SD, Standard Deviation; ALBI, albumin-bilirubin grade; HBV, hepatitis B virus; AFP, alpha-fetoprotein; ALT, alanine transaminase; AST, aspartate aminotransferase; PT, prothrombin time; ALB, albumin blood; TBIL, total bilirubin; IQ, interquartile.

Table 2 Preoperative Predictors for ER in the Training and the Validation Sets

Characteristic	Training Set (n=138)			Validation Set (n=35)		
	ER (n=55)	Non-ER (n=83)	P-value	ER (n=14)	Non-ER (n=21)	P-value
Sex			0.070			0.128
Male	47 (85.5)	60 (72.3)		13 (92.9)	15 (71.4)	
Female	8 (14.5)	23 (27.7)		1 (7.1)	6 (28.6)	
Age (years, mean ± SD)	57.47 ± 10.45	55.78 ± 10.44	0.351	57.25 ± 11.11	58.91 ± 10.21	0.512
Maximum tumor diameter (cm, mean ± SD)	5.60 ± 2.87	4.61 ± 2.87	0.046	5.59 ±3.66	4.92 ±3.62	0.014
ALBI grade			0.091			0.786
I	16 (29.1)	36 (43.4)		6 (42.9)	8 (38.1)	
II	39 (70.9)	47 (56.6)		8 (57.1)	13 (61.9)	
HBV			0.489			0.339
Positive	37 (67.3)	51 (61.4)		7 (50)	14 (66.7)	
Negative	18 (32.7)	32 (38.6)		7 (50)	7 (33.3)	
Cirrhosis			0.136			0.422
Positive	29 (52.7)	33 (39.8)		8 (57.1)	9 (42.9)	
Negative	26 (47.3)	50 (60.2)		6 (42.9)	12 (57.1)	
AFP (ng/mL)			0.187			0.699
≤20	22 (40)	45 (54.2)		4 (28.6)	9 (42.9)	
20–400	13 (23.6)	13 (15.7)		5 (35.7)	4 (19)	
≥400	20 (36.4)	25 (30.1)		5 (35.7)	8 (38.1)	
ALT (U/L, mean ± SD)	41.89 ± 28.18	45.74 ± 43.20	0.561	66.71 ± 73.67	46.95 ± 43.68	0.326
AST (U/L, mean ± SD)	41.00 ±19.08	32.43 ± 14.70	0.004	71.00 ± 70.14	31.38 ± 16.19	0.017
PT (s, mean ± SD)	12.00 ± 0.95	12.28 ± 2.04	0.351	11.59 ± 0.86	11.82 ± 1.22	0.566
ALB (g/L, mean ± SD)	38.20 ± 3.87	38.86 ± 3.86	0.328	38.84 ± 3.40	39.14 ± 2.88	0.776
TBIL (μmol/L, mean ± SD)	17.45 ± 7.41	13.85 ± 6.35	0.003	20.38 ± 13.82	12.61 ± 4.08	0.020
HCC Rad_score (medians ± IQ)	0.47 ± 0.18	0.31 ± 0.14	<0.001	0.52 ± 0.26	0.28 ± 0.18	<0.001
Spleen Rad_score (medians ± IQ)	0.42 ± 0.06	0.36 ± 0.06	<0.001	0.46 ± 0.09	0.34 ±0.08	0.001
Combined Rad_score (medians ± IQ)	0.63 ± 0.43	0.24 ± 0.27	<0.001	0.75 ± 0.36	0.19 ± 0.29	<0.001

Note: Data are numbers of patients and parentheses indicate the proportion if not specified.
Abbreviations: ER, Early recurrence; SD, standard deviation; ALBI, albumin-bilirubin grade; AFP, alpha fetoprotein; ALT, alanine transaminase; PT, prothrombin time; ALB, albumin blood; TBIL, total bilirubin; IQ, interquartile.

Selection of Radiomics Features and Construction of Prediction Model

Three thousand eight hundred twelve radiomics features were extracted from the HCC and spleen images of each patient. For the tumor and spleen regions, the number of features with ICC greater than 0.75 after intra- and inter-rater robustness testing were 2714 and 3192, respectively. The reproducibility of the extracted features is shown in Figure S1. The rad-scores of the two regions, HCC Rad_score and Spleen Rad_score, were established by LASSO Cox regression analysis. The HCC Rad_score contains eight arterial phase features and seven venous phase features. The spleen Rad_score had five arterial phase features and four venous phase features, and the weights of the features included in each region are shown in Figure 2. The LASSO Cox regression procedure is shown in Figure S2. The formulae for the two rad-scores are detailed in Appendix 1. After constructing the rad-scores for HCC and the spleen, we built a two-region joint model using logistic regression and calculated the combined Rad_score for all patients.

Verification and Comparison of Three Radiological Characteristics

We plotted ROC curves to evaluate the predictive performance of the three rad-scores for ER. The results showed that the HCC and spleen joint models achieved excellent predictive value, with an AUC of 0.853 (95% CI, 0.783–0.908) in the development cohort (Figure 3A). Similar results were observed in the validation cohort. The joint HCC and spleen model yielded a high AUC of 0.929 (95% CI, 0.789–0.988) (Figure 3B). Moreover, the joint model accuracy, specificity, and PPV were > 80.0% in the two cohorts (Table 3). The DeLong test was performed on the ROC curves of the three models among the

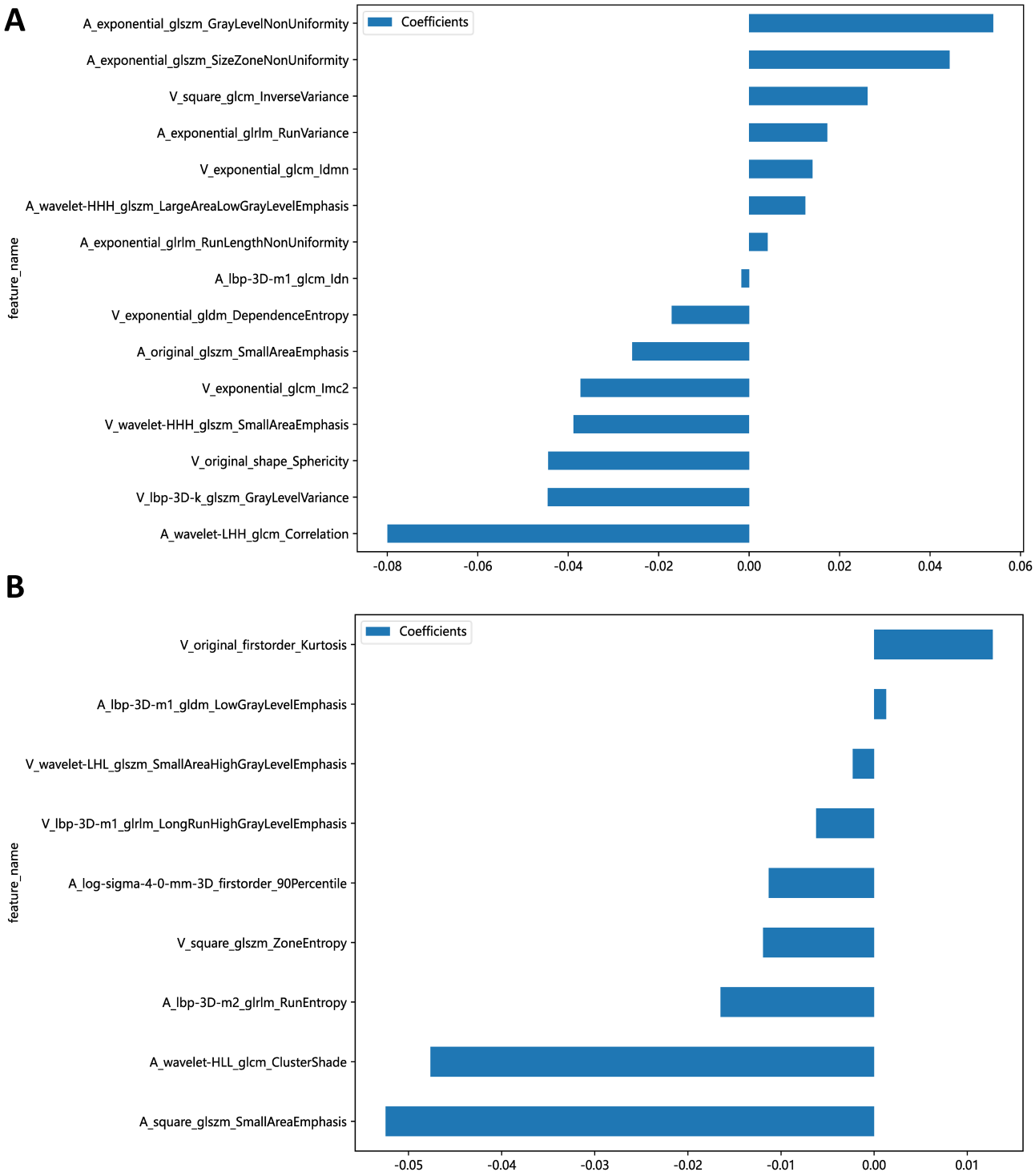

Figure 2 The weights of the features contained in HCC (**A**) and spleen (**B**). The classification and interpretation for radiomics features were listed in Table S2.

AUCs values in the training cohort. The differences between the joint model with HCC and the spleen were statistically significant ($p = 0.0202$ and $p = 0.0027$, respectively) (Table S1). Two cases with familiar clinical information were selected for comparison to demonstrate the predictive ability of the model based on ER radiomics. The results showed that the two presented HCC patients, who had distinctly different ER statuses (Case1 ER, Case2 non-ER) with similar clinicopathological features showed significantly different combined Rad_scores (0.96 vs 0.13; $p < 0.001$) (Figure 4).

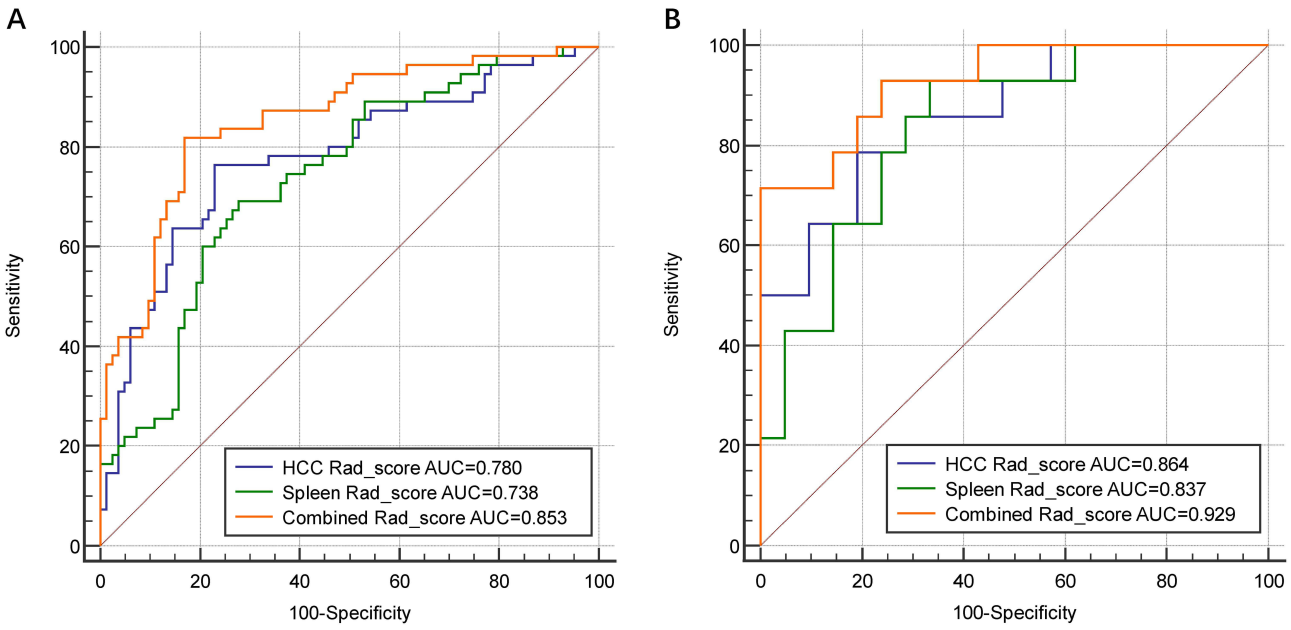

Figure 3 ROC curves of three prediction models to predict ER in PA-TACE patients. (**A**) Training set; (**B**) validation set.

Modeling and Evaluation of the Radiomics Nomogram

TBIL and combined Rad_score were identified as independent risk predictors for assessing ER in patients with HCC using multivariate logistic regression analysis (Table 4). Based on this, we constructed a radiomic nomogram combining TBIL levels (Figure 5A). ROC curves were plotted to evaluate the predictive performance of radiomics combined with the clinical features of ER. Both the training and validation sets demonstrated good predictive performance with an AUC test of 0.88 (95% CI, 0.82 to 0.94) and 0.95 (95% CI, 0.87 to 1.00) (Figure 5B and C). The nomogram calibration curves are shown in Figures 5D and E. These curves indicate that the nomogram achieved better agreement between predicted survival and observed outcomes. The ER prediction decision curves shown in Figure 5F, and G demonstrate the clinical utility of the prediction model, suggesting that a significant overall net benefit can be obtained for the nomogram over most threshold probability ranges. Finally, we divided the patients into high- and low-risk groups in the training and validation sets using the median score of nomograms (cut-off value: 0.296) as the cut-off. Based on this, CICs were plotted (Figure 5H and I). The CIC curves further showed that the model predicted the ER probability after a risk level of >20%, which is in good agreement with the actual ER probability.

Table 3 Predictive Performances of Three Radiomics Scores for Predicting ER Probability

Signature	AUC	Sensitivity	Specificity
HCC Rad_score			
Training set	0.780	76.36	77.11
Validation set	0.864	78.57	80.95
Spleen Rad_score			
Training set	0.738	69.09	72.29
Validation set	0.837	92.86	66.67
Combined Rad_score			
Training set	0.853	81.82	83.13
Validation set	0.929	71.43	79.25

Abbreviations: ER, early recurrence; AUC, area under curve; HCC, hepatocellular carcinoma.

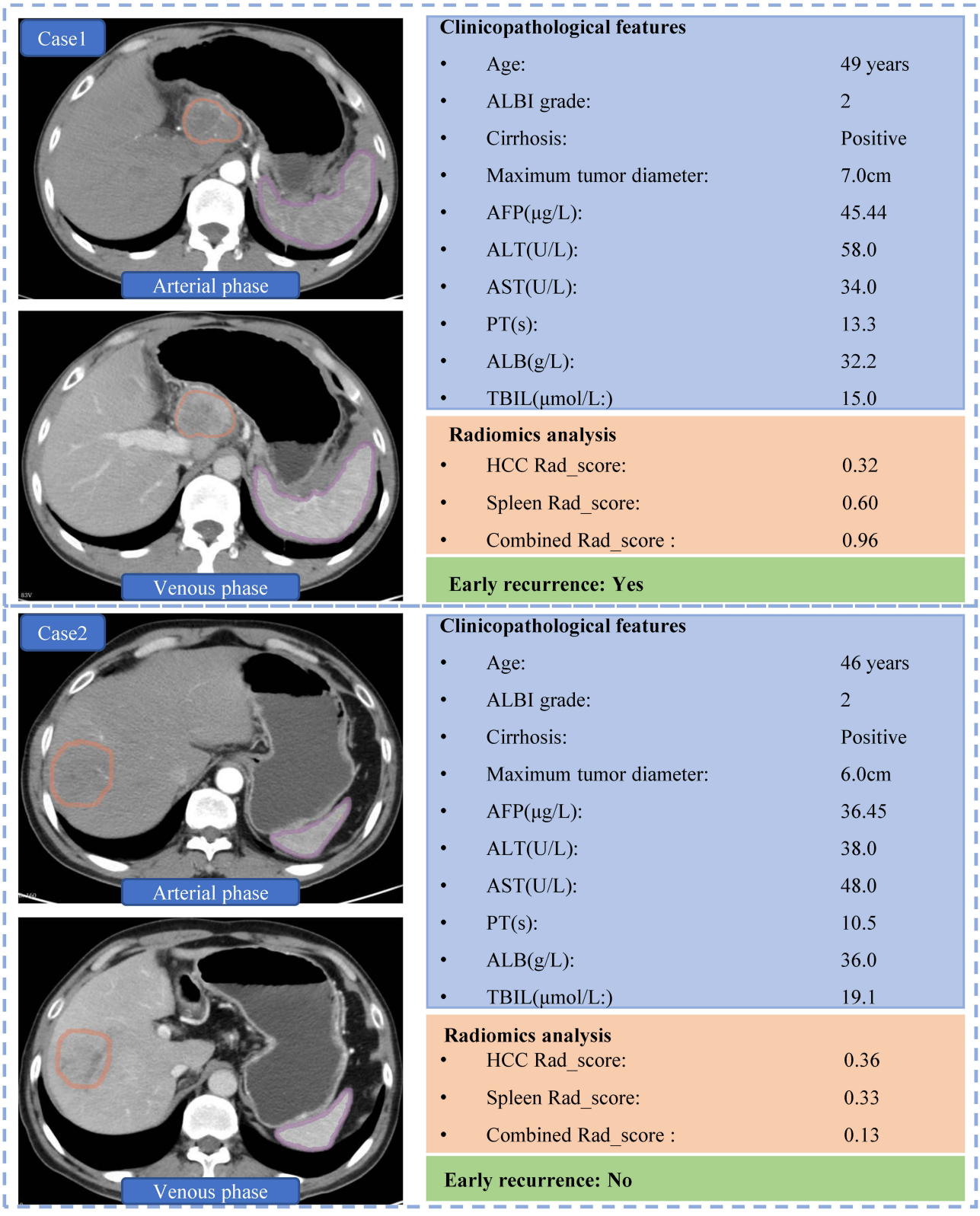

Figure 4 Two presented cases of PA-TACE patients who had distinctly different relapse situations with similar clinicopathological features showed significantly different combined Rad_score (0.96 vs 0.13, p<0.001). In the left CT scan image, the region delineated by the Orange contour represents the area of the liver tumor, while the region delineated by the purple contour represents the area of the spleen. Both contours were manually drawn.

Table 4 Statistical Analysis of Meaningful Preoperative Predictors for ER

Intercept and Variable	Coefficient	Std. Error	Odds Ratio (95% CI)	P-value
Maximum tumor diameter	−0.11076	0.088931	0.8952 (0.7520 to 1.0656)	0.213
AST	0.027212	0.015	1.0276 (0.9978 to 1.0582)	0.070
TBIL	0.10204	0.037375	1.1074 (1.0292 to 1.1916)	0.006
Combined Rad_score	0.62209	0.10871	1.8628 (1.5053 to 2.3052)	<0.001

Note: Parentheses indicate 95% confidence interval.
Abbreviations: Std. Error, Standard error; AST, aspartate transaminase; TBIL, total bilirubin.

Discussion

Postoperative adjuvant therapy for HCC is aimed at reducing recurrence. The Chinese guidelines for the diagnosis and treatment of primary liver cancer (2022 edition) consider PA-TACE to reduce recurrence and prolong survival for patients with high-risk factors such as surgically resected tumor diameter over 5 cm, multiple nodes, poorly defined HCC, and microvascular invasion (MVI).[26] Some studies believe that PA-TACE can improve the prognosis of patients with HCC by using lipiodol via microvascular embolization to treat small tumor lesions or hidden intrahepatic multifocal HCC that cannot be detected by traditional imaging methods.[29,30] In addition, several papers reported that PA-TACE can delay the recurrence time and reduce the recurrence rate of HCC after surgery.[31–33] PA-TACE is one of the methods used to prevent the recurrence of hepatocellular carcinoma after surgical resection, but many patients still experience ER after PA-TACE. Indicators such as routine blood tests, liver function, and tumor markers tested during postoperative follow-up cannot accurately predict recurrence in patients. Therefore, identifying indicators that can predict recurrence in PA-TACE patients has become an urgent clinical problem. Nowadays, radiomics aims to predict the diagnosis and prognosis of HCC by extracting and analyzing quantitative features from various imaging modalities such as ultrasound (US), CT, magnetic resonance imaging (MRI), and positron emission tomography/CT (PET/CT). Hu et al extracted features from contrast-enhanced ultrasound images to predict microvascular invasion in patients with HCC prior to surgery.[34] Zhang et al extracted radiomic features from gadolinium ethoxybenzyl diethylenetriamine pentaacetic acid-enhanced MRI and constructed nomograms for predicting microvascular invasion in patients with solitary HCC ≤5 cm.[35] Li et al combined radiomics features from 18F-FDG PET/CT (D-PET/CT model) and clinical-pathological features to predict the status of microvascular invasion in patients with very early and early-stage (BCLC 0, BCLC A) HCC.[36] Because of the advantages of noninvasive, simple, and fast imaging, predictive models of PA-TACE patient prognosis based on imaging are also emerging.[37] However, we found that almost all models were based on the imaging data of HCC before hepatectomy, which may have missed some critical imaging features. The spleen is a crucial organ detected on abdominal CT scans. As an essential lymphoid organ, the spleen can regulate innate and acquired immunity and promote tumor progression and metastasis by influencing immunosuppression.[22,23] One study reported that CT-based radiomic features of the spleen could predict the prognosis of patients with gastric cancer.[24] Spleen volume and stiffness measurements were independent predictors of prognosis in response to HCC.[38,39] The above findings suggest that spleen-related imaging features may respond to some extent to the progression of tumors, primarily hepatocellular carcinoma. In this study, we innovatively constructed a multimodal two-region imaging omics model using CT images of HCC and the spleen to predict the ER status in patients undergoing PA-TACE. Encouragingly, a dual-target combination model combining radiological and clinical pathology features showed better prognostic performance and clinical utility than single-region models. The nomograms obtained in this study can easily be used to calculate patient ER probability, thus helping in selecting the timing of initial surgery and PA-TACE.

According to the clinical practice of transarterial chemoembolization for hepatocellular carcinoma, the evaluation of TACE was divided into short-term and long-term effects.[10] The Japanese Society of Hepatology (JSH)-liver cancer research group (LCSGJ) considered that TACE resistance could be judged by the presence of more than 50% residual activity or new lesions on CT/MRI 1–3 months after two or more consecutive TACE treatments.[40] If tumor progression occurs after TACE, TACE treatment can continue if the patient's liver function allows it until the patient cannot benefit.[41] Owing to the short interval and frequency of PA-TACE after hepatectomy, PA-TACE benefits patients in the short term. Therefore, assessing the probability of ER in patients undergoing PA-TACE has far-reaching implications in the selection of subsequent treatments. Apart from TACE, systemic therapies including targeted therapy and immunotherapy have become standard treatment options for patients with

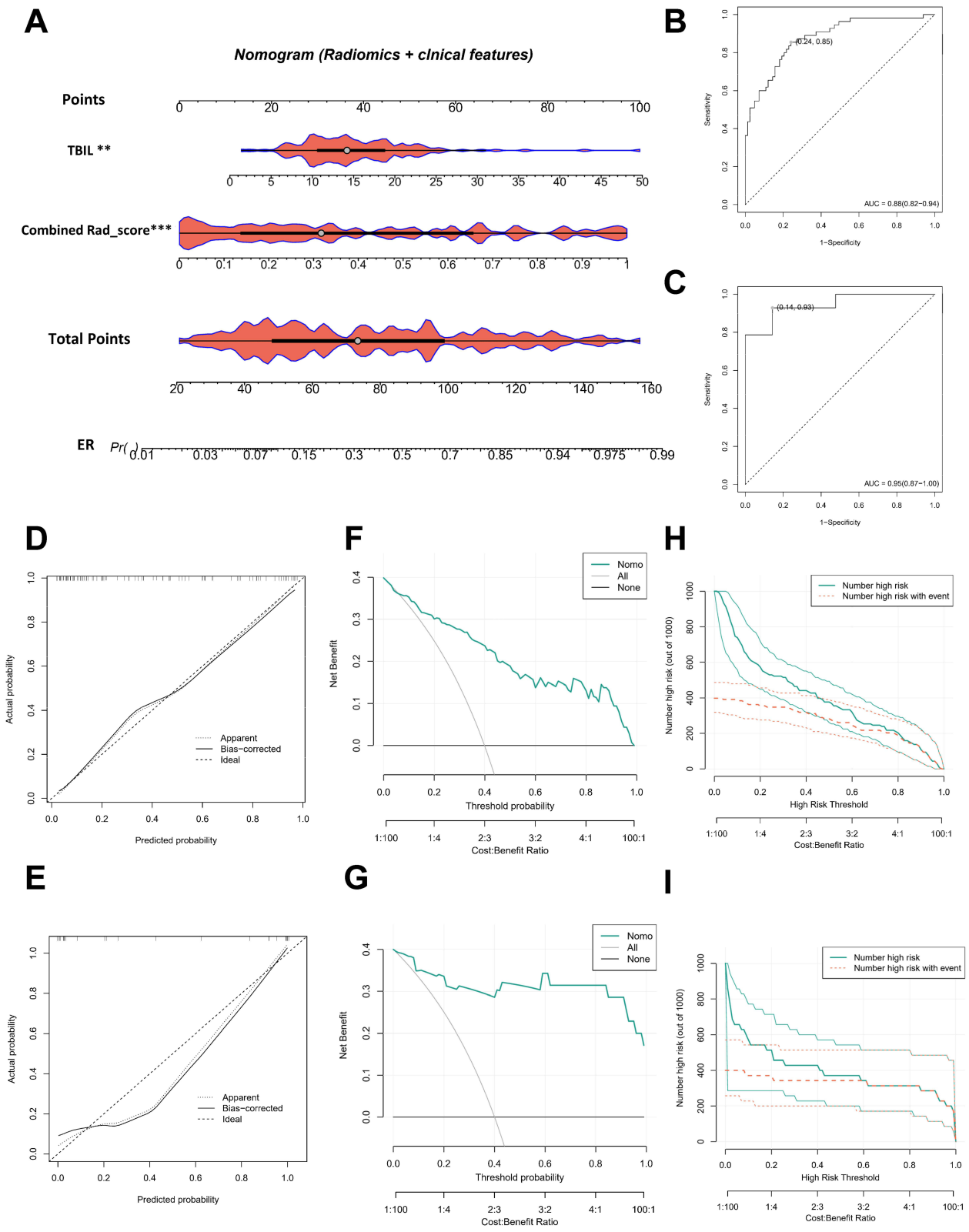

Figure 5 Radiomics nomogram for ER prediction and its assessment. Radiomics nomogram combining the TBIL level and combined Rad_score (**A**) ROC curves of radiomics nomogram in training (**B**) and validation (**C**) sets. Calibration curve of radiomics nomogram in training (**D**) and validation (**E**) sets. Decision curve analysis of radiomics nomogram in training (**F**) and validation (**G**) sets. Clinical impact curve of radiomics nomogram in training (**H**) and validation (**I**) sets.

advanced HCC. Recent studies have shown that combining TACE with targeted immunotherapy can prolong patients' survival.[8,42] Currently, targeted drugs used in HCC treatment mainly consist of multi-target tyrosine kinase inhibitors, while immunotherapy primarily involves the use of PD-1 and PD-L1 inhibitors.[43] The combination of TACE and systemic therapy holds promising prospects for HCC treatment.

In the present study, we performed multivariate analysis of clinical information and radiomics features, which revealed that the combined Rad_score was an independent prognostic factorfor predicting ER after PA-TACE in HCC patients. TBIL is the sum of direct and indirect bilirubin levels and accurately reflects the degree of jaundice, indicating liver function status.[44] TBIL was reported to be able to predict the recurrence of HCC in patients with Child grade A.[45] TBIL is an independent predictor of survival in patients with spontaneously ruptured HCC.[46,47] Based on the multivariate analysis results, we established and validated a nomogram containing radiomic and clinical information to predict ER after PA-TACE in patients with HCC alone. This nomogram achieved better results (AUC) in both training and validation sets. This study investigated the predictive value of dual-region radiomic features on the prognosis of patients with HCC undergoing PA-TACE after radical surgery. The predictive performance of the nomogram consisting of dual-region radiomic features and clinical risk factors was evaluated. Two patients with similar clinical characteristics were selected to highlight the unique predictive performance of the dual-region radiomic profile. Clinical information (including age, ABIL classification, history of cirrhosis, tumor size, AFP, ALT, AST, PT, ALB, and TBIL) was similar in both patients, yet the ER status of the two patients was the opposite. Patients with ER had a higher combined Rad score than those without ER. At the end of the study, we divided the patients into high- and low-risk groups using the median score of the nomogram (cut-off value, 0.296) as a cut-off. Based on this, we plotted CIC. The results indicated that the nomogram had high clinical efficiency.

Our study has some limitations. This was a retrospective single-center study with heterogeneity in patient populations, imaging methods, and possible selection bias. We provide antiviral treatment and monitor treatment efficacy for patients confirmed to have hepatitis B virus infection, but the lack of prior awareness of the infection among most HCC patients hinders the collection and analysis of data related to hepatitis B treatment. This limitation affects the investigation of antiviral treatment's role in ER after PA-TACE. There may be data overfitting owing to the small sample size. Future studies will require a larger cohort to validate our results. Finally, owing to the lack of rich clinical information collected in this study, it was impossible to construct a valid predictive model based on clinical information for comparison with radiomic features. Hopefully, this aspect can be remedied in the future by upgrading hospital management systems.

Conclusion

In summary, we developed a non-invasive predictive nomogram. The nomogram, which combines the radiological features of HCC and spleen multimodality CT imaging with clinical risk factors, can effectively predict the ER status in patients undergoing PA-TACE and guide more appropriate surgical plans.

Data Sharing Statement

The original contributions presented in the study are included in the article and its Supplementary Materials. Further inquiries can be directed to the corresponding authors.

Ethics Statement

This retrospective study, conducted at the Affiliated Hospital of Nantong University, was approved by the Ethics Committee (approval number: 2022-K090-01, approval date: 24 July 2022). Informed consent from patients was waived by the committee, considering the retrospective nature of the study and the utilization of anonymized data, while ensuring patient privacy and confidentiality. All patient data were handled in strict accordance with relevant privacy regulations, guidelines, and the principles outlined in the Declaration of Helsinki, ensuring confidentiality and anonymity throughout the study.

Acknowledgments

We thank the China Postdoctoral Foundation and the National Natural Science Foundation of China for financial support.

Author Contributions

All authors made a significant contribution to the work reported, whether that is in the conception, study design, execution, acquisition of data, analysis and interpretation, or in all these areas; took part in drafting, revising or critically reviewing the article; gave final approval of the version to be published; have agreed on the journal to which the article has been submitted; and agree to be accountable for all aspects of the work.

Funding

This research was funded by the National Natural Science Foundation of China (82272093), the Young Scientists Fund of the National Natural Science Foundation of China (82102167) and China Postdoctoral Science Foundation (2019M651928).

Disclosure

The authors declare that the research was conducted in the absence of any commercial or financial relationships that could be construed as a potential conflict of interest.

References

1. Sung H, Ferlay J, Siegel RL, et al. Global cancer statistics 2020: GLOBOCAN estimates of incidence and mortality worldwide for 36 cancers in 185 countries. *CA Cancer J Clin*. 2021;71(3):209–249. doi:10.3322/caac.21660
2. Ferlay J, Soerjomataram I, Dikshit R, et al. Cancer incidence and mortality worldwide: sources, methods and major patterns in GLOBOCAN 2012. *Int J Cancer*. 2015;136(5):E359–86. doi:10.1002/ijc.29210
3. Cabibbo G, Enea M, Attanasio M, Bruix J, Craxi A, Camma C. A meta-analysis of survival rates of untreated patients in randomized clinical trials of hepatocellular carcinoma. *Hepatology*. 2010;51(4):1274–1283. doi:10.1002/hep.23485
4. Madkhali AA, Fadel ZT, Aljiffry MM, Hassanain MM. Surgical treatment for hepatocellular carcinoma. *Saudi J Gastroenterol*. 2015;21(1):11–17. doi:10.4103/1319-3767.151216
5. Tabrizian P, Jibara G, Shrager B, Schwartz M, Roayaie S. Recurrence of hepatocellular cancer after resection: patterns, treatments, and prognosis. *Ann Surg*. 2015;261(5):947–955. doi:10.1097/SLA.0000000000000710
6. Han K, Kim JH. Transarterial chemoembolization in hepatocellular carcinoma treatment: Barcelona clinic liver cancer staging system. *World J Gastroenterol*. 2015;21(36):10327–10335. doi:10.3748/wjg.v21.i36.10327
7. Heimbach JK, Kulik LM, Finn RS, et al. AASLD guidelines for the treatment of hepatocellular carcinoma. *Hepatology*. 2018;67(1):358–380. doi:10.1002/hep.29086
8. European Association for the Study of the Liver. Electronic address eee, European Association for the Study of the L. EASL clinical practice guidelines: management of hepatocellular carcinoma. *J Hepatol*. 2018;69(1):182–236. doi:10.1016/j.jhep.2018.03.019
9. Sun Y, Zhang W, Bi X, et al. Systemic therapy for hepatocellular carcinoma: Chinese consensus-based interdisciplinary expert statements. *Liver Cancer*. 2022;11(3):192–208. doi:10.1159/000521596
10. Lu J, Zhao M, Arai Y, et al. Clinical practice of transarterial chemoembolization for hepatocellular carcinoma: consensus statement from an international expert panel of International Society of Multidisciplinary Interventional Oncology (ISMIO). *Hepatobiliary Surg Nutr*. 2021;10 (5):661–671. doi:10.21037/hbsn-21-260
11. Cheng H, Yang X, Liu G. Superstable homogeneous iodinated formulation technology: revolutionizing transcatheter arterial chemoembolization. *Sci Bull*. 2020;65(20):1685–1687. doi:10.1016/j.scib.2020.06.029
12. Li Z, Cheng H, Mao J, Liu G. Conversion therapy of intermediate and advanced hepatocellular carcinoma using superstable homogeneous iodinated formulation technology. *Sci China Life Sci*. 2022;65(10):2114–2117. doi:10.1007/s11427-022-2142-3
13. Wang H, Du PC, Wu MC, Cong WM. Postoperative adjuvant transarterial chemoembolization for multinodular hepatocellular carcinoma within the Barcelona clinic liver cancer early stage and microvascular invasion. *Hepatobiliary Surg Nutr*. 2018;7(6):418–428. doi:10.21037/hbsn.2018.09.05
14. Chen X, Zhang B, Yin X, Ren Z, Qiu S, Zhou J. Lipiodolized transarterial chemoembolization in hepatocellular carcinoma patients after curative resection. *J Cancer Res Clin Oncol*. 2013;139(5):773–781. doi:10.1007/s00432-012-1343-7
15. Poon RT, Fan ST, Lo CM, Liu CL, Wong J. Intrahepatic recurrence after curative resection of hepatocellular carcinoma: long-term results of treatment and prognostic factors. *Ann Surg*. 1999;229(2):216–222. doi:10.1097/00000658-199902000-00009
16. Poon RT, Fan ST, Ng IO, Lo CM, Liu CL, Wong J. Different risk factors and prognosis for early and late intrahepatic recurrence after resection of hepatocellular carcinoma. *Cancer*. 2000;89(3):500–507. doi:10.1002/1097-0142(20000801)89:3<500::AID-CNCR4>3.0.CO;2-O
17. Lambin P, Leijenaar RTH, Deist TM, et al. Radiomics: the bridge between medical imaging and personalized medicine. *Nat Rev Clin Oncol*. 2017;14(12):749–762. doi:10.1038/nrclinonc.2017.141
18. Gillies RJ, Kinahan PE, Hricak H. Radiomics: images are more than pictures, they are data. *Radiology*. 2016;278(2):563–577. doi:10.1148/radiol.2015151169
19. Zhou Y, He L, Huang Y, et al. CT-based radiomics signature: a potential biomarker for preoperative prediction of early recurrence in hepatocellular carcinoma. *Abdom Radiol*. 2017;42(6):1695–1704.
20. Guo D, Gu D, Wang H, et al. Radiomics analysis enables recurrence prediction for hepatocellular carcinoma after liver transplantation. *Eur J Radiol*. 2019;117:33–40. doi:10.1016/j.ejrad.2019.05.010
21. Brenet Defour L, Mule S, Tenenhaus A, et al. Hepatocellular carcinoma: CT texture analysis as a predictor of survival after surgical resection. *Eur Radiol*. 2019;29(3):1231–1239. doi:10.1007/s00330-018-5679-5
22. Lewis SM, Williams A, Eisenbarth SC. Structure and function of the immune system in the spleen. *Sci Immunol*. 2019;4(33):1.

23. Han Y, Liu Q, Hou J, et al. Tumor-induced generation of splenic erythroblast-like ter-cells promotes tumor progression. *Cell*. 2018;173(3):634–48 e12. doi:10.1016/j.cell.2018.02.061
24. Wang X, Sun J, Zhang W, et al. Use of radiomics to extract splenic features to predict prognosis of patients with gastric cancer. *Eur J Surg Oncol*. 2020;46(10 Pt A):1932–1940. doi:10.1016/j.ejso.2020.06.021
25. Huang YS, Chen XD, Shi MM, et al. Diffuse reduction of spleen density is an independent predictor of post-operative outcomes after curative gastrectomy in gastric cancer: a multi-center study. *Front Oncol*. 2020;10:1050. doi:10.3389/fonc.2020.01050
26. Bureau of Medical Administration. 原发性肝癌诊疗指南 (2022年版) [Standardization for diagnosis and treatment of hepatocellular carcinoma (2022 edition)]. *Zhonghua Gan Zang Bing Za Zhi*. 2022;30(4):367–388. Chinese.
27. Clinical Guidelines Committee of Chinese Interventionalists C. 中国肝细胞癌经动脉化疗栓塞(TACE)治疗临床实践指南 (2021年版) [Chinese clinical practice guidelines for transarterial chemoembolization of hepatocellular carcinoma]. *Zhonghua Nei Ke Za Zhi*. 2021;60(7):599–614. Chinese. doi:10.3760/cma.j.cn112137-20210425-00991
28. Lencioni R, Llovet JM. Modified RECIST (mRECIST) assessment for hepatocellular carcinoma. *Semin Liver Dis*. 2010;30(1):52–60. doi:10.1055/s-0030-1247132
29. Wang Z, Ren Z, Chen Y, et al. Adjuvant transarterial chemoembolization for HBV-related hepatocellular carcinoma after resection: a randomized controlled study. *Clin Cancer Res*. 2018;24(9):2074–2081.
30. Aufhauser DD, Sadot E, Murken DR, et al. Incidence of occult intrahepatic metastasis in hepatocellular carcinoma treated with transplantation corresponds to early recurrence rates after partial hepatectomy. *Ann Surg*. 2018;267(5):922–928. doi:10.1097/SLA.0000000000002135
31. Rodriguez-Peralvarez M, Luong TV, Andreana L, Meyer T, Dhillon AP, Burroughs AK. A systematic review of microvascular invasion in hepatocellular carcinoma: diagnostic and prognostic variability. *Ann Surg Oncol*. 2013;20(1):325–339.
32. Chen ZH, Zhang XP, Zhou TF, et al. Adjuvant transarterial chemoembolization improves survival outcomes in hepatocellular carcinoma with microvascular invasion: a systematic review and meta-analysis. *Eur J Surg Oncol*. 2019;45(11):2188–2196. doi:10.1016/j.ejso.2019.06.031
33. Zhang XP, Chai ZT, Gao YZ, et al. Postoperative adjuvant sorafenib improves survival outcomes in hepatocellular carcinoma patients with microvascular invasion after R0 liver resection: a propensity score matching analysis. *HPB*. 2019;21(12):1687–1696. doi:10.1016/j.hpb.2019.04.014
34. Hu HT, Wang Z, Huang XW, et al. Ultrasound-based radiomics score: a potential biomarker for the prediction of microvascular invasion in hepatocellular carcinoma. *Eur Radiol*. 2019;29(6):2890–2901. doi:10.1007/s00330-018-5797-0
35. Chong HH, Yang L, Sheng RF, et al. Multi-scale and multi-parametric radiomics of gadoxetate disodium-enhanced MRI predicts microvascular invasion and outcome in patients with solitary hepatocellular carcinoma </= 5 cm. *Eur Radiol*. 2021;31(7):4824–4838. doi:10.1007/s00330-020-07601-2
36. Li Y, Zhang Y, Fang Q, et al. Radiomics analysis of [(18)F]FDG PET/CT for microvascular invasion and prognosis prediction in very-early- and early-stage hepatocellular carcinoma. *Eur J Nucl Med Mol Imaging*. 2021;48(8):2599–2614. doi:10.1007/s00259-020-05119-9
37. Liu F, Guo X, Dong W, et al. Postoperative adjuvant TACE-associated nomogram for predicting the prognosis of resectable Hepatocellular carcinoma with portal vein tumor thrombus after liver resection. *Int J Biol Sci*. 2020;16(16):3210–3220. doi:10.7150/ijbs.46896
38. Marasco G, Colecchia A, Colli A, et al. Role of liver and spleen stiffness in predicting the recurrence of hepatocellular carcinoma after resection. *J Hepatol*. 2019;70(3):440–448. doi:10.1016/j.jhep.2018.10.022
39. Takeishi K, Kawanaka H, Itoh S, et al. Impact of splenic volume and splenectomy on prognosis of hepatocellular carcinoma within Milan criteria after curative hepatectomy. *World J Surg*. 2018;42(4):1120–1128. doi:10.1007/s00268-017-4232-z
40. Kudo M, Kawamura Y, Hasegawa K, et al. Management of Hepatocellular carcinoma in Japan: JSH consensus statements and recommendations 2021 update. *Liver Cancer*. 2021;10(3):181–223. doi:10.1159/000514174
41. Chang Y, Jeong SW, Young Jang J, Jae Kim Y. Recent updates of transarterial chemoembolilzation in Hepatocellular carcinoma. *Int J Mol Sci*. 2020;21(21):8165. doi:10.3390/ijms21218165
42. Reig M, Forner A, Rimola J, et al. BCLC strategy for prognosis prediction and treatment recommendation: the 2022 update. *J Hepatol*. 2022;76(3):681–693. doi:10.1016/j.jhep.2021.11.018
43. Yang F, Deng K, Zheng H, Liu Z, Zheng Y. Progress of targeted and immunotherapy for hepatocellular carcinoma and the application of next-generation sequencing. *Ann Hepatol*. 2022;27(2):100677. doi:10.1016/j.aohep.2022.100677
44. Zelenka J, Lenicek M, Muchova L, et al. Highly sensitive method for quantitative determination of bilirubin in biological fluids and tissues. *J Chromatogr B Analyt Technol Biomed Life Sci*. 2008;867(1):37–42. doi:10.1016/j.jchromb.2008.03.005
45. Wu B, Hu X, Jin H, et al. Albumin-bilirubin and platelet-albumin-bilirubin grades for hepatitis B-associated hepatocellular carcinoma in Child-Pugh A patients treated with radical surgery: a retrospective observational study. *Medicine*. 2019;98(43):e17394. doi:10.1097/MD.0000000000017394
46. Wang P, Moses AS, Li C, et al. Prognosis factors of predicting survival in spontaneously ruptured hepatocellular carcinoma. *Hepatol Int*. 2022;16:1330–1338. doi:10.1007/s12072-022-10403-x
47. Zou J, Yuan J, Chen H, et al. Development of a prognostic score for recommended transarterial chemoembolization candidates with spontaneous rupture of hepatocellular carcinoma. *J Gastrointest Oncol*. 2022;13(3):1376–1383. doi:10.21037/jgo-22-531